Supplementary Information (SI) for New Journal of Chemistry.
This journal is © The Royal Society of Chemistry and the Centre National de la Recherche Scientifique 2024

NDI-BODIPY-Graphene Oxide Nanosized Photocatalysts for LED Irradiated Organic Synthesis

Hande Eserci Gürbüz[a], Ezel Öztürk Gündüz[a], Ümmügülsüm Büyükpolat[a], Elif Okutan[a*]

[a] Department of Chemistry, Faculty of Science, Gebze Technical University, Gebze, Kocaeli, Türkiye

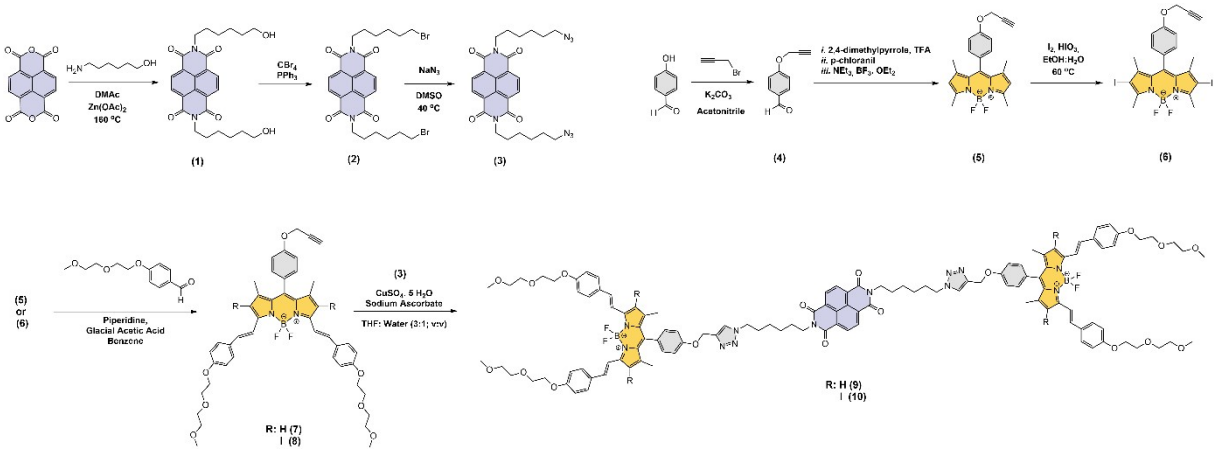

Scheme S1: Synthetic route of compounds **1-10.**

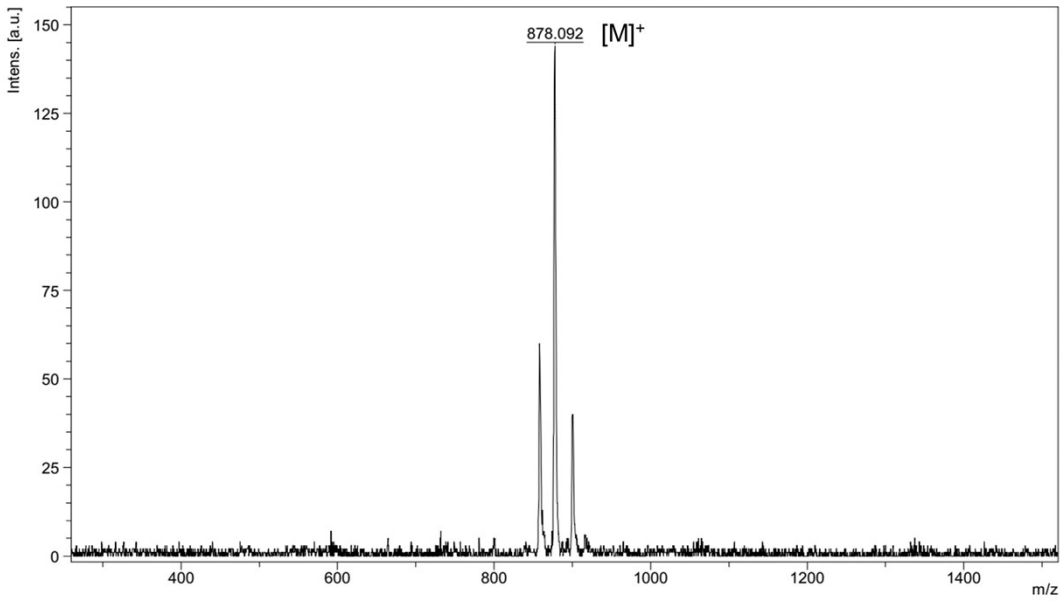

Fig. S1 MALDI-MS spectrum of compound **7**.

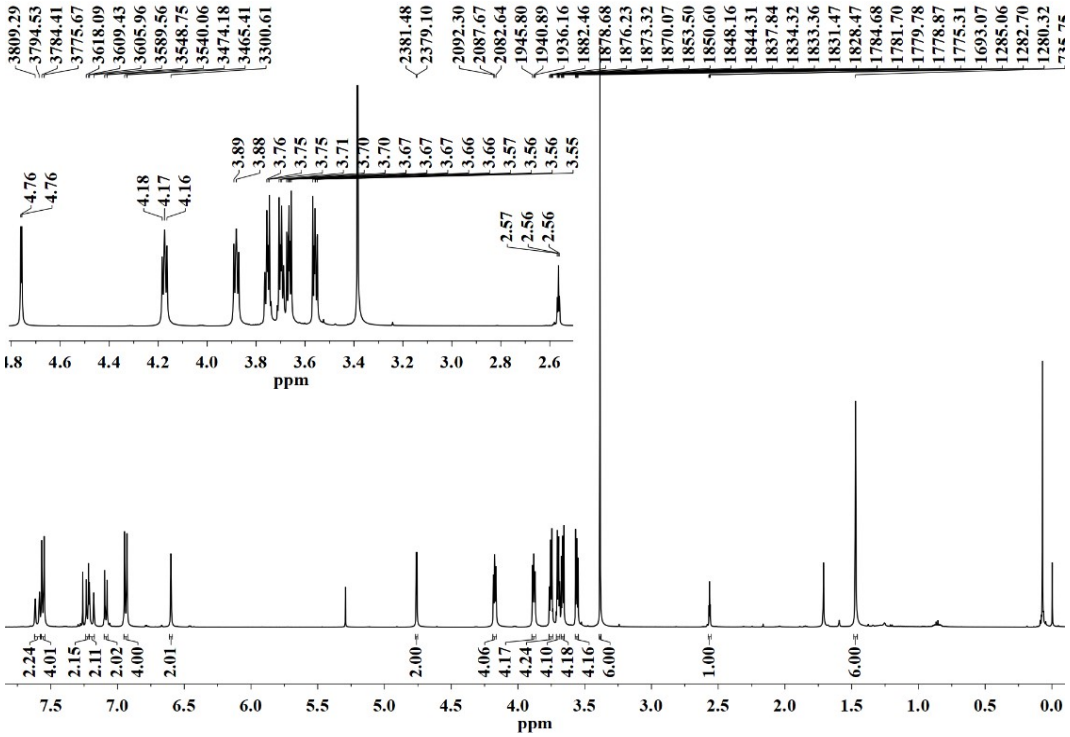

Fig. S2 ^{1}H NMR spectrum of compound **7**.

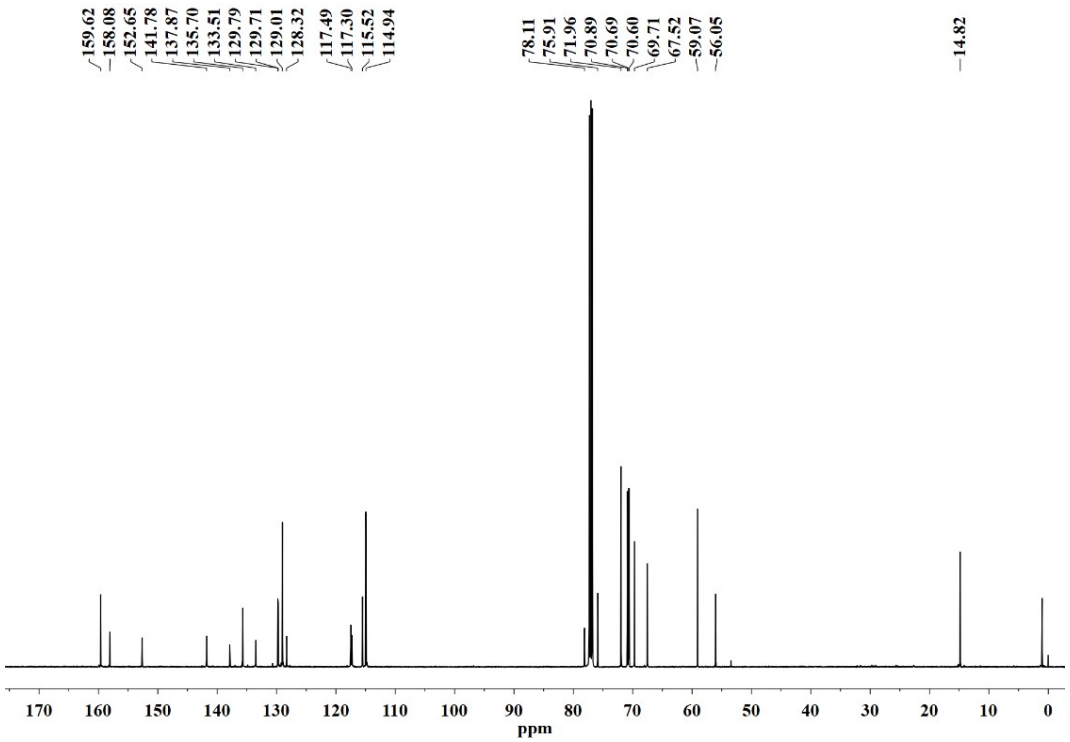

Fig. S3 ^{13}C NMR spectrum of compound **7**.

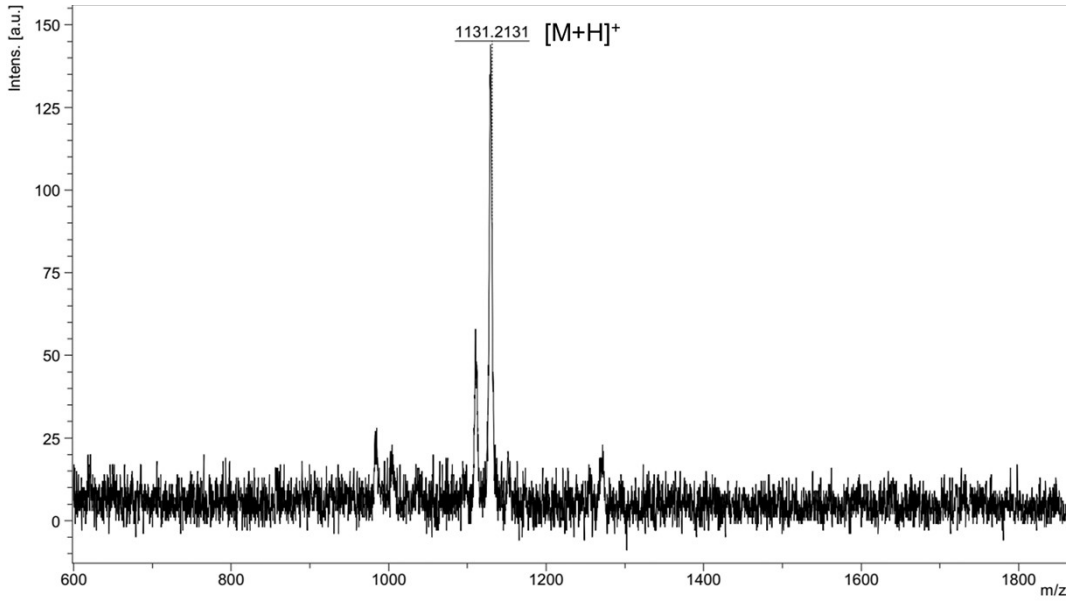

Fig. S4 MALDI-MS spectrum of compound **8**.

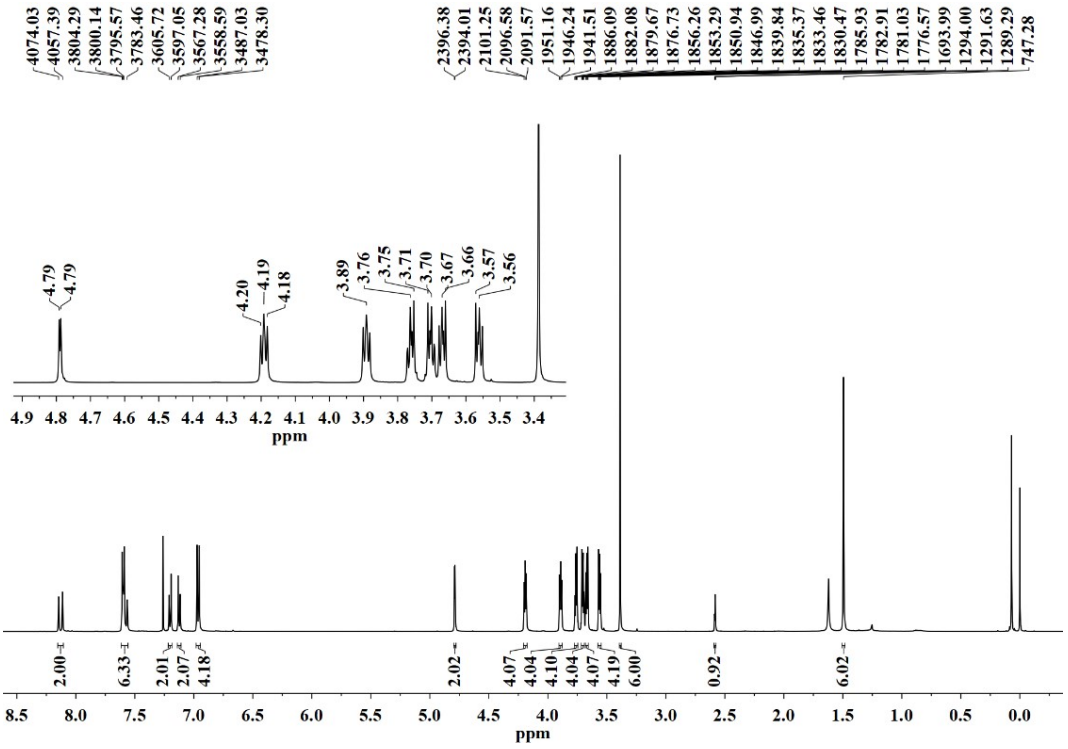

Fig. S: 5 H NMR spectrum of compound **8**.

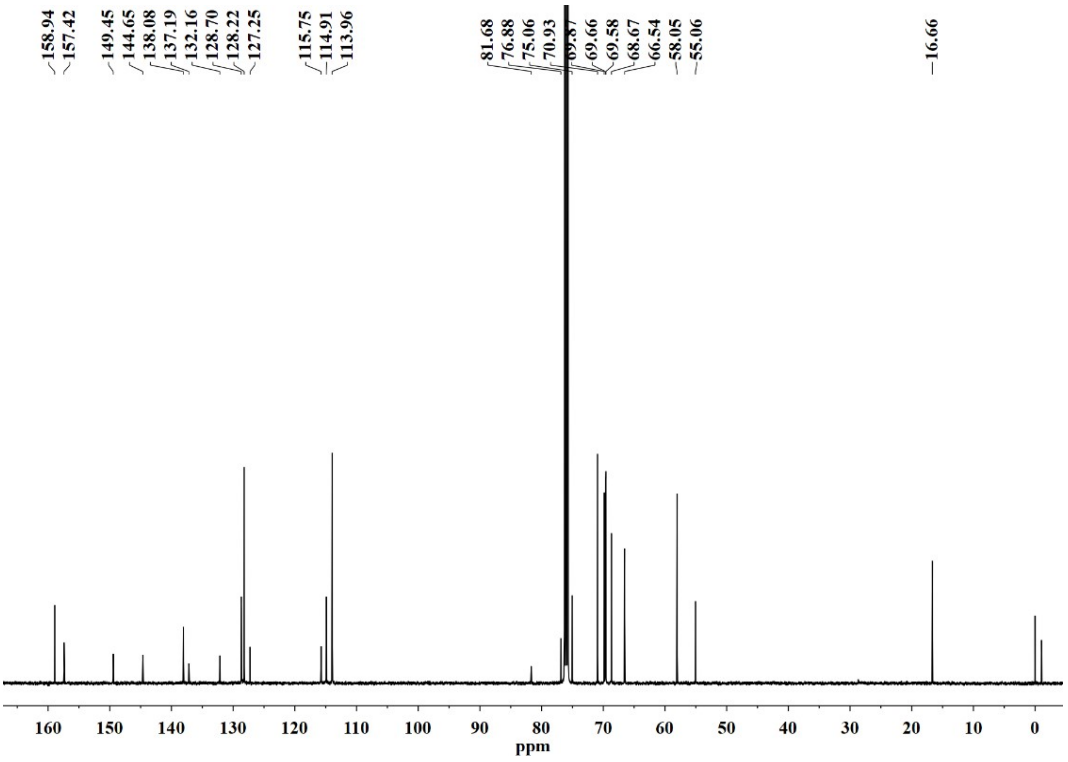

Fig. S6 ^{13}C NMR spectrum of compound **8**.

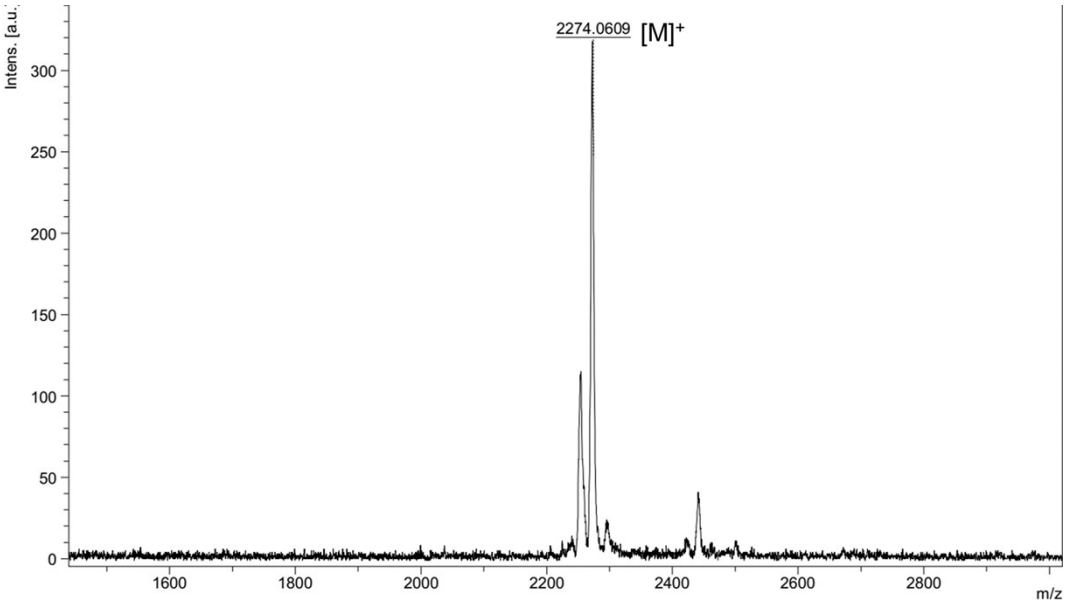

Fig. S7 MALDI-MS spectrum of compound **9**.

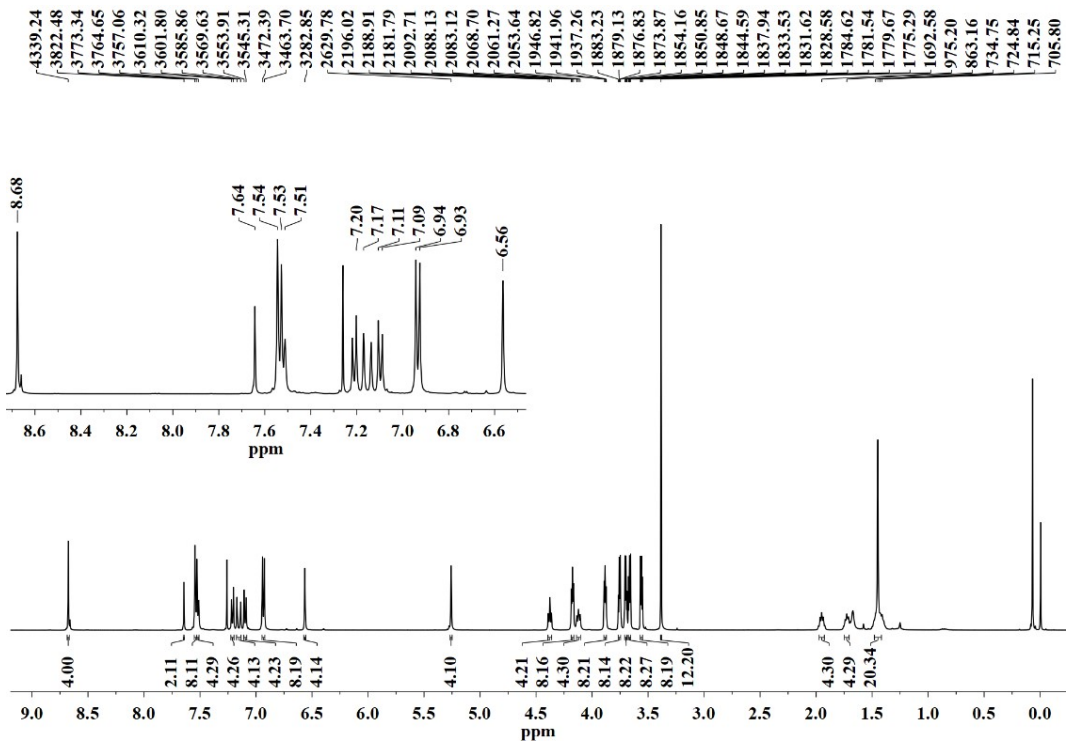

Fig. S8 ^{1}H NMR spectrum of compound **9**.

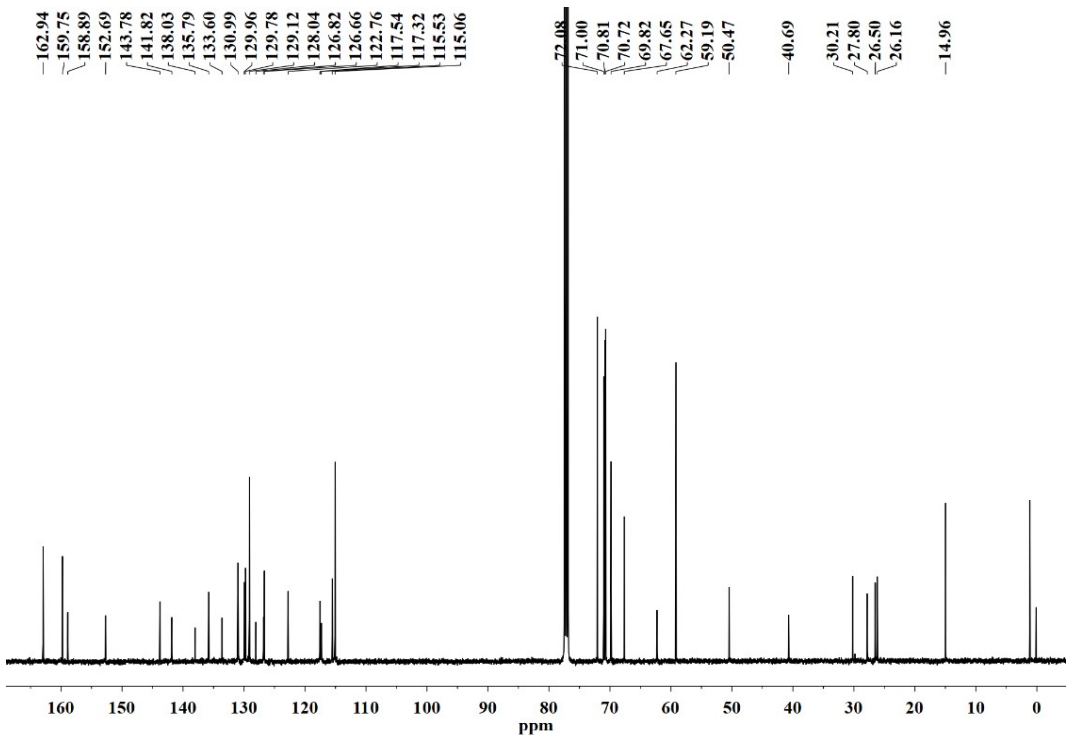

Fig. S9 ^{13}C NMR spectrum of compound **9**.

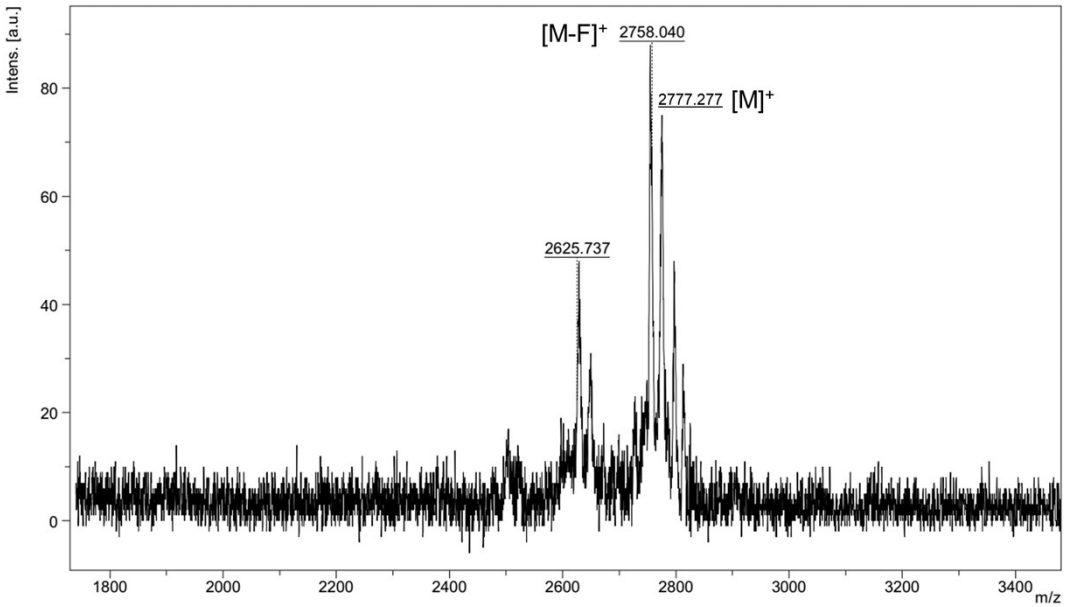

Fig. S10 MALDI-MS spectrum of compound **10**.

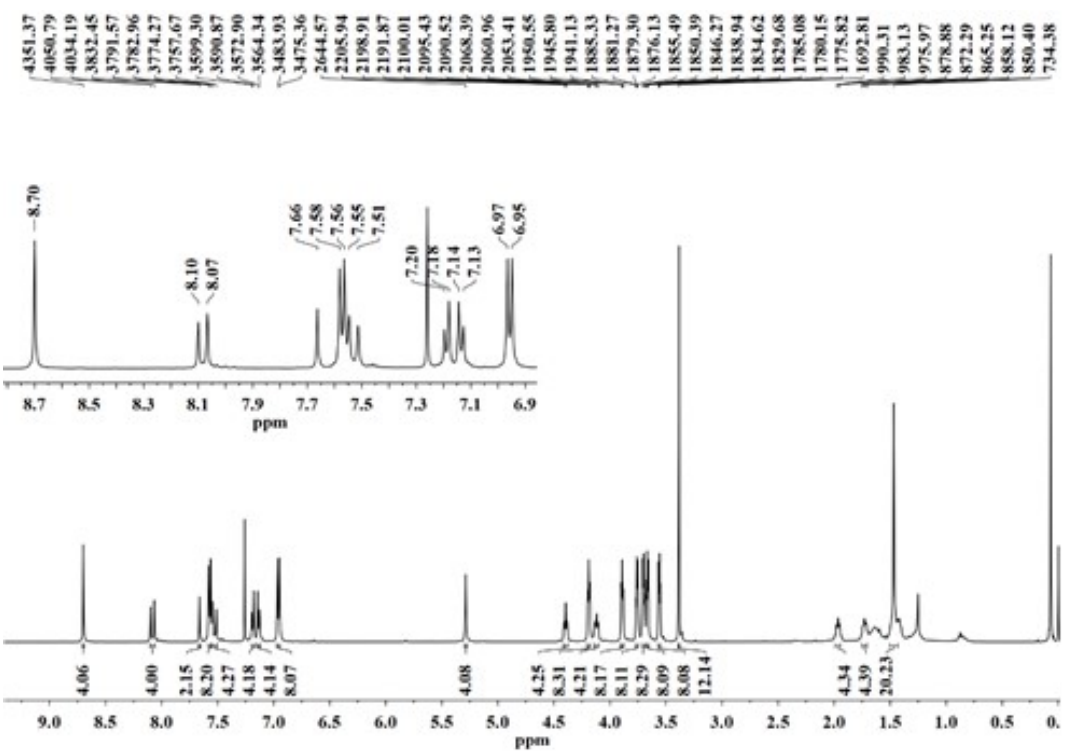

Fig. S11 ^{1}H NMR spectrum of compound **10**.

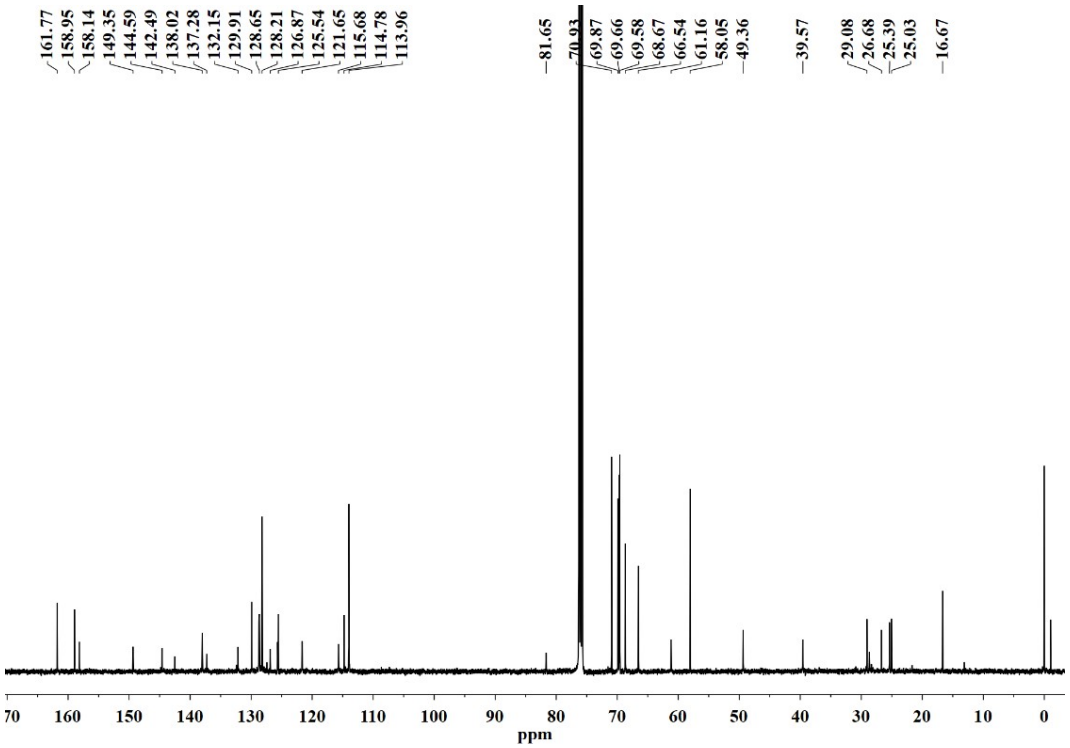

Fig. S12 ^{13}C NMR spectrum of compound **10**.

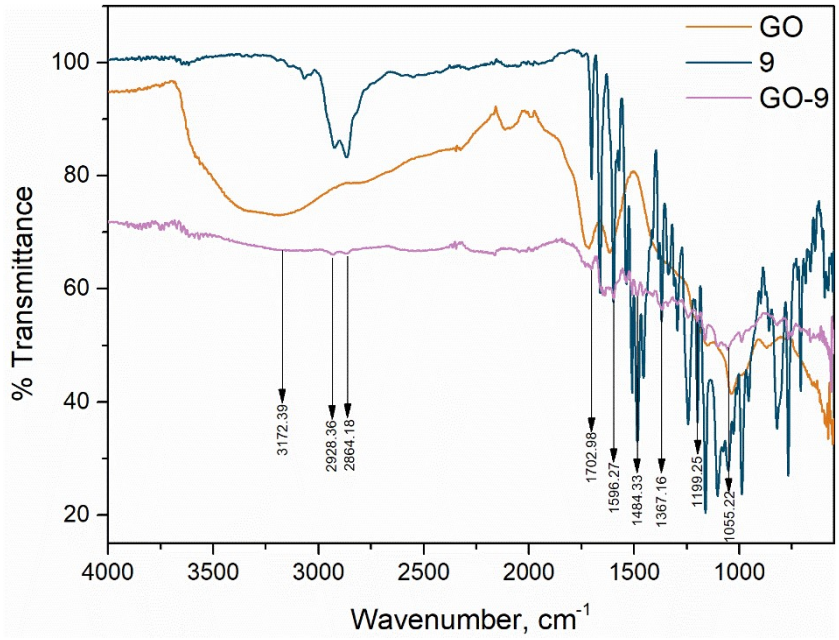

Fig. S13 Overlay FT-IR spectra of **GO**, compound **9** and **GO-9**.

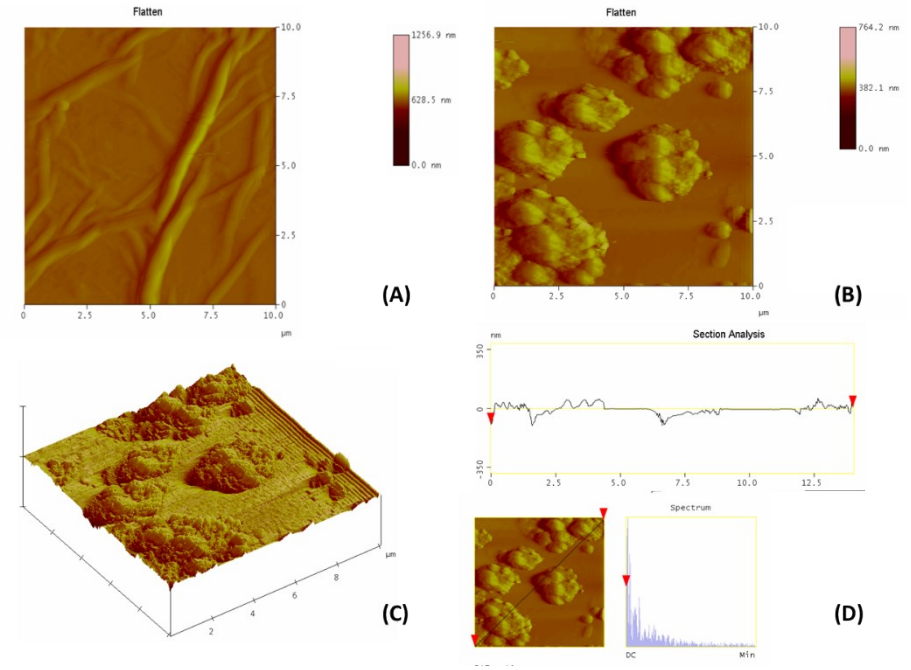

Fig. S14 2D AFM images of (A) **GO** and (B) **GO-9**, (C) 3D AFM image of **GO-9** and (D) cross-sectional analysis of **GO-9**.

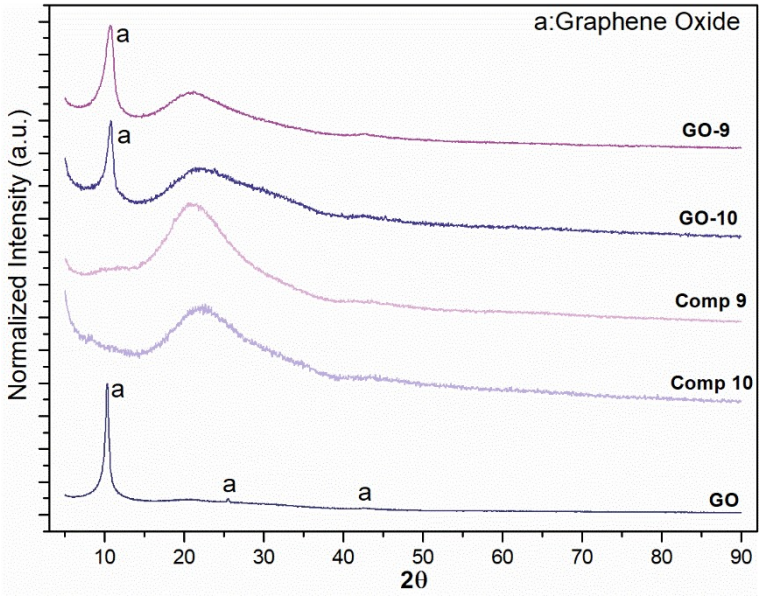

Fig. S15 XRD Diffractogram of **GO**, compounds **9**, **10** and nanocomposites **GO-9** and **GO-10**.

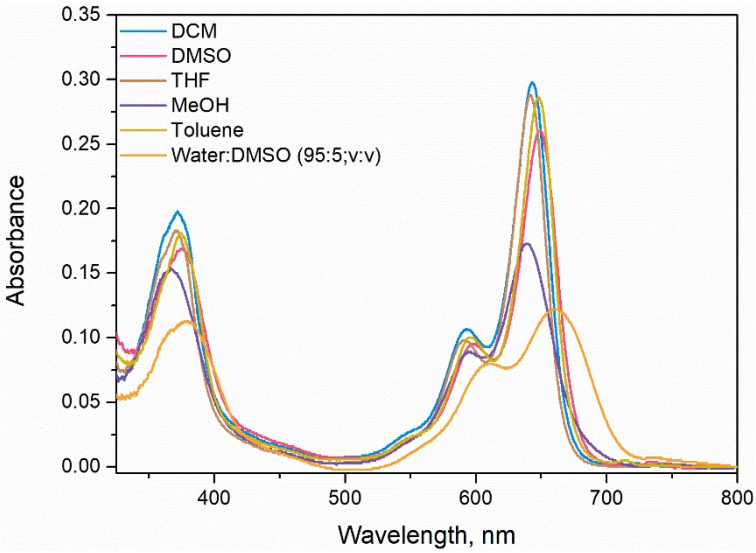

Fig. S16 UV-Vis absorption spectra of compound **9** in different solvents at 1 μM.

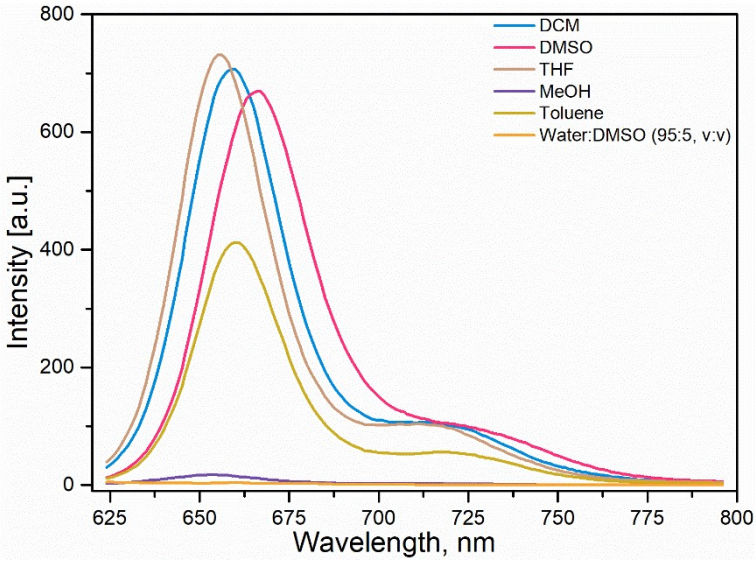

Fig. S17 Fluorescence spectra of compound **9** in different solvents at 1 μM (λ_{ex}:610nm).

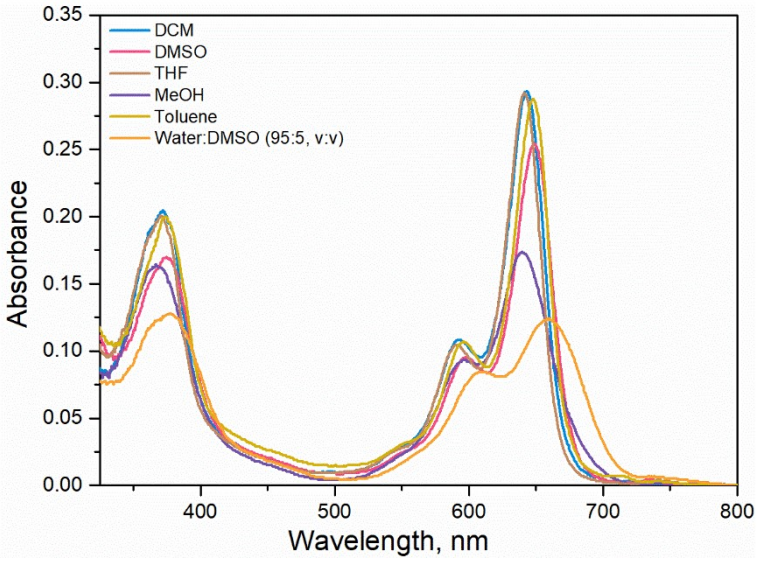

Fig. S18 UV-Vis absorption spectra of **GO-9** in different solvents at 1 μM.

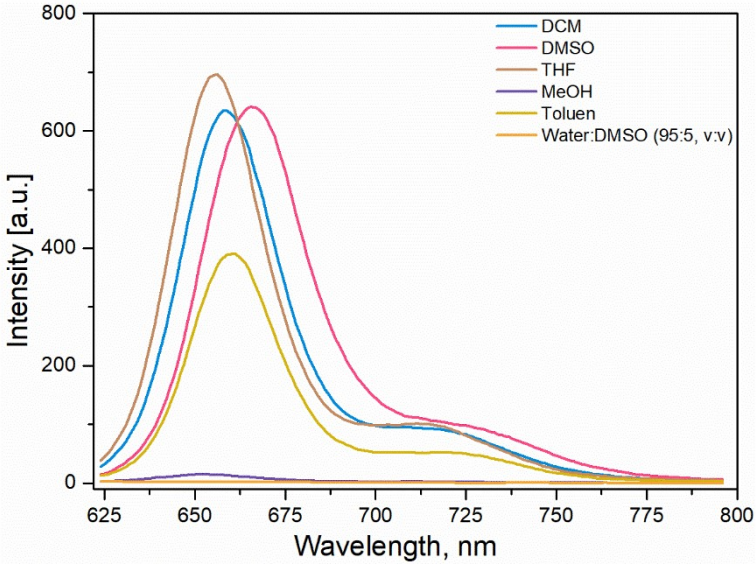

Fig. S19 Fluorescence spectra of **GO-9** in different solvents at 1 μM (λ_{ex}:610nm).

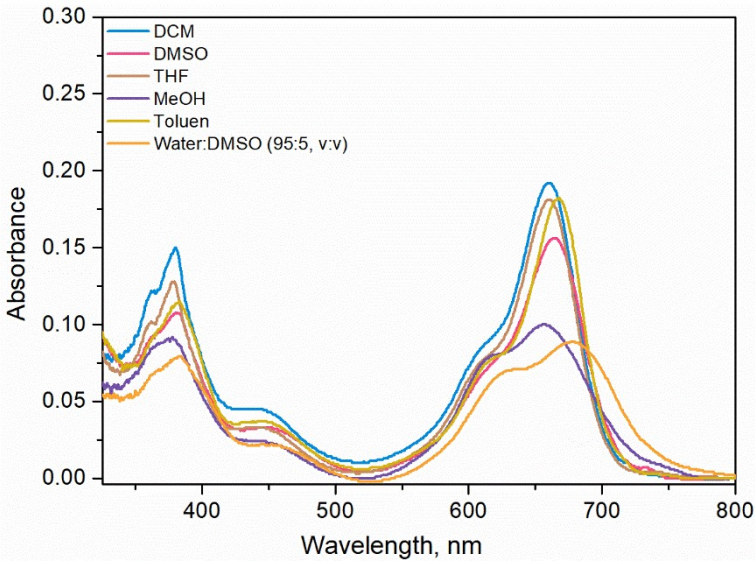

Fig. S20 UV-Vis absorption spectra of compound **10** in different solvents at 1 µM.

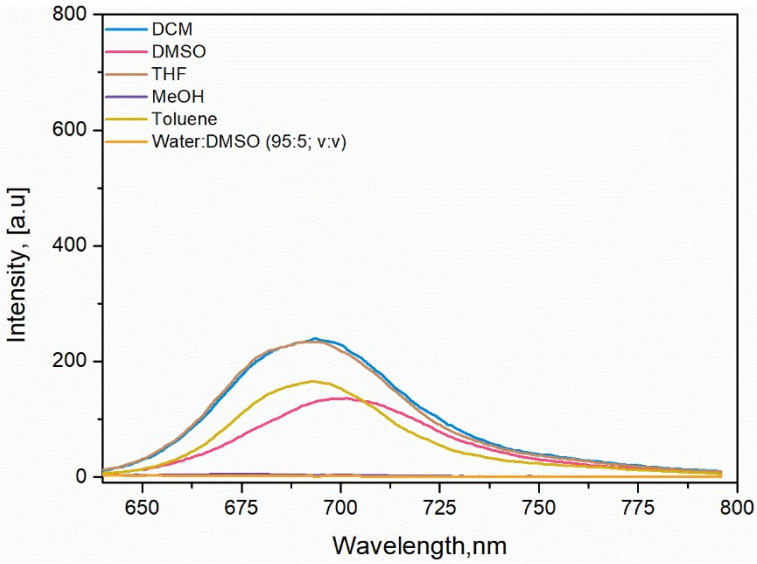

Fig. S21 Fluorescence spectra of compound **10** in different solvents at 1 µM (λ_{ex}:620nm).

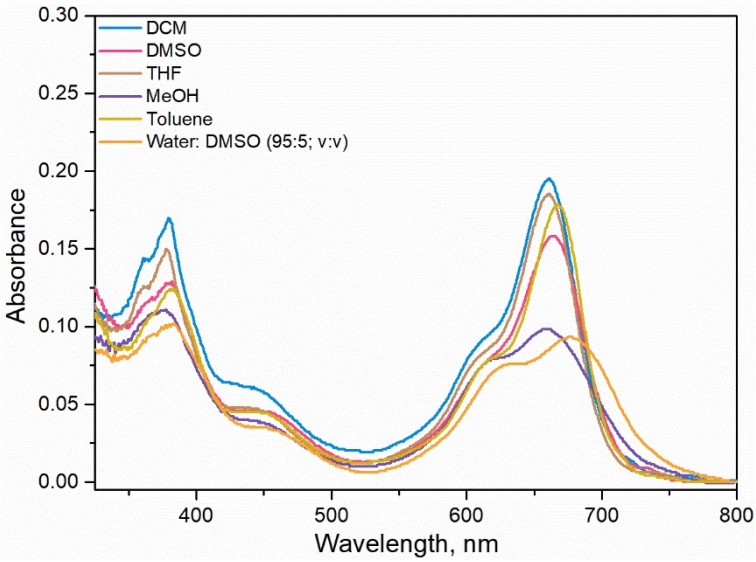

Fig. S22 UV-Vis absorption spectra of **GO-10** in different solvents at 1 μM.

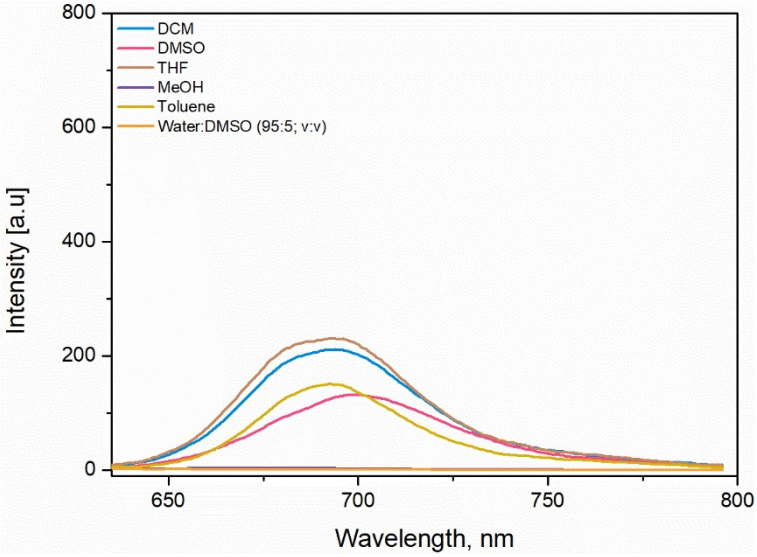

Fig. S23 Fluorescence spectra of **GO-10** in different solvents at 1 μM (λ_{ex}:620nm).

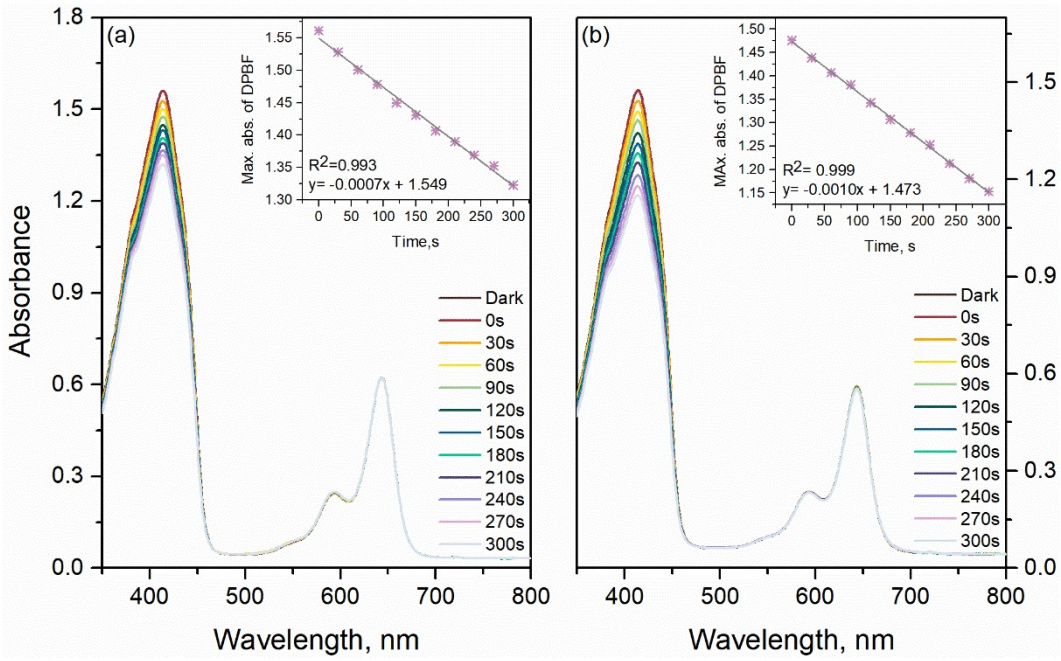

Fig. S24 Absorbance decrease of DPBF in the presence of 2 μM a) compound **9** and b) **GO-9**.

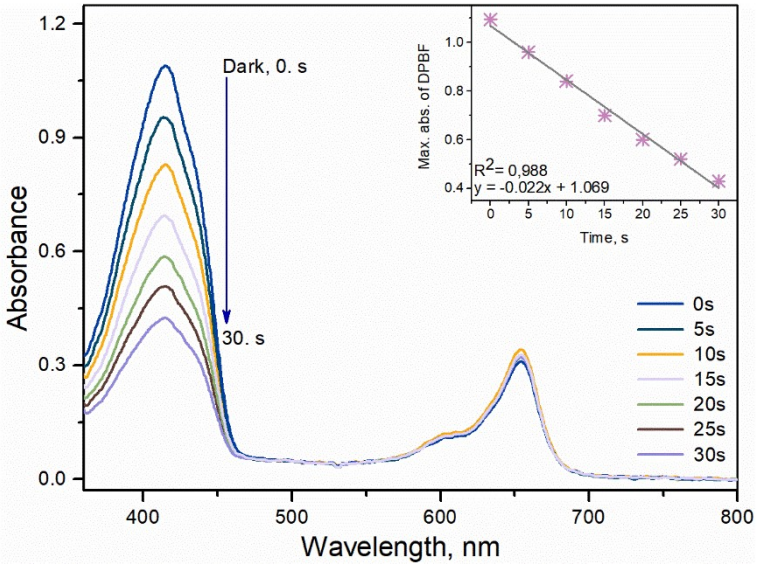

Fig. S25 Absorbance decrease of DPBF in the presence of 2 μM methylene blue.

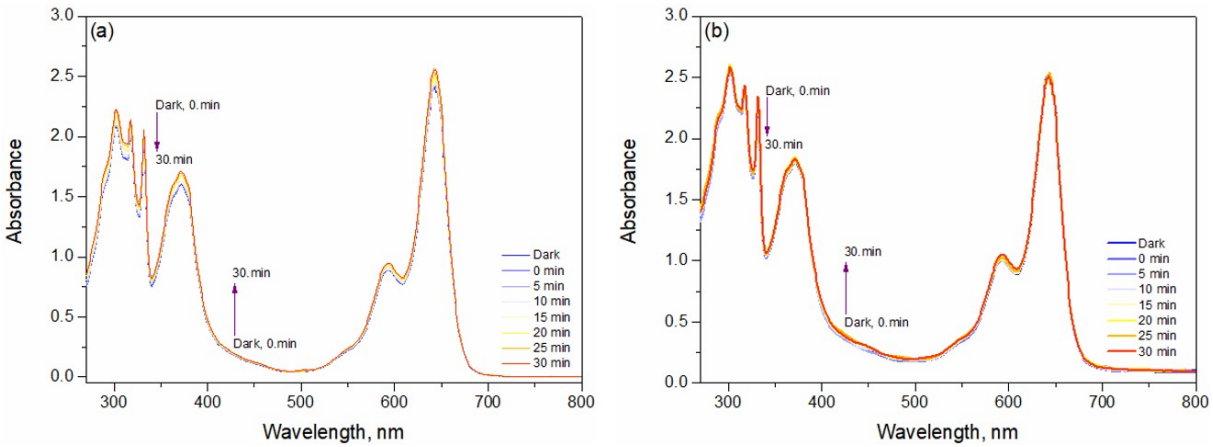

Fig. S26 UV-vis absorption spectra of a) **9** and b) **GO-9** containing DHN

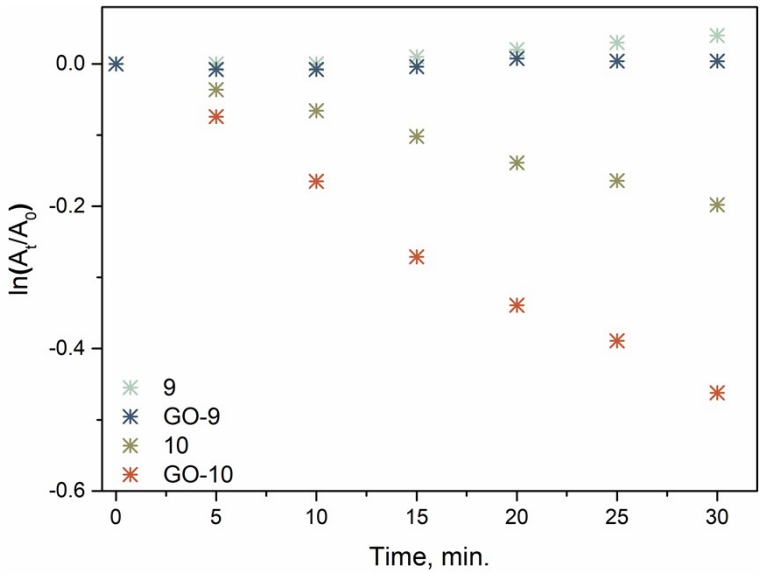

Fig. S27 Plots of $\ln(A_t/A_0)$ vs. irradiation time (t) for the photooxidation of DHN.

Table S1. ^{1}H NMR Parameters of compounds **7-10**.

	N-CH	**Ar-CH**	***trans*-CH**	**pyrrole-CH**	**-NCH_2**	**$H_2C{\equiv}C$**	**-OCH_2**	**-OCH_3**	**C≡CH**	**-CH_2-**	**-CH_3**
7	-	• 7.56 (d, 4H) *J*= 8.7 Hz • 7.23 (d, 2H) *J*= 8.7 Hz • 7.09 (d, 2H) *J*= 8.7 Hz • 6.94 (d,4H), *J*= 8.8 Hz	• 7.60 (d, 2H) *J*= 14.8 Hz • 7.19 (d, 2H) *J*= 16.4 Hz	6.60 (s, 2H)	-	4.76 (d, 2H) *J*= 2.4 Hz	• 4.17 (t, 4H) *J*= 4.8 Hz • 3.88 (t, 4H) *J*= 4.8 Hz • 3.76-3.74 (m, 4H) • 3.71-3.69 (m, 4H) • 3.68-3.65 (m, 4H) • 3.57-3.55 (m, 4H)	3.39 (s, 6H)	2.56 (t, 1H) *J*= 2.4 Hz	-	1.47 (s, 6H)
8	-	• 7.60 (d, 4H) *J*= 8.7 Hz • 7.20 (d, 2H) *J*= 8.7 Hz • 7.12 (d, 2H) *J*= 8.7 Hz • 6.96 (d, 4H) *J*= 8.7 Hz	• 8.13 (d, 2H) *J*= 16.6 Hz • 7.58 (d, 2H) *J*= 16.7 Hz	-	-	4.79 (d, 2H) *J*= 2.4 Hz	• 4.19 (t, 4H) *J*= 4.8 Hz, • 3.89 (t, 4H) *J*= 4.8 Hz • 3.77-3.75 (m, 4H) • 3.71- 3.69 (m,4H) • 3.68-3.66 (m, 4H) • 3.57-3.55 (m, 4H)	3.39 (s, 6H)	2.58 (t, 1H) *J*= 2.4 Hz	-	1.49 (s, 6H)
9	7.64 (s, 2H)	• 8.68 (s, 4H) • 7.53 (d, 8H) *J*= 8.7 Hz • 7.21 (d, 4H) *J*= 8.5 Hz • 7.10 (d, 4H) *J*= 8.6 Hz • 6.93 (d, 8H) *J*= 8.7 Hz	• 7.52 (d, 4H) *J*= 16.3 Hz • 7.15 (d, 4H) *J*= 16.2 Hz	6.56 (s, 4H)	• 4.38 (t, 4H) *J*= 7.1 Hz • 4.12 (t, 4H) *J*= 7.5 Hz	-	• 5.26 (s, 4H) • 4.17 (t, 8H) *J*= 4.8 Hz • 3.88 (t, 8H) *J*= 4.8 Hz • 3.76-3.74 (m, 8H) • 3.71-3.69 (m, 8H) • 3.67-3.66 (m, 8H) • 3.57-3.55 (m, 8H)	3.38 (s, 12H)	-	• 1.95 (q, 4H) *J*= 7.2 Hz • 1.73 (q, 4H) *J*= 7.4 Hz	1.45 (m, 20H)
10	7.66 (s, 2H)	• 8.70 (s, 4H) • 7.57 (d, 8H) *J*= 8.6 Hz • 7.19 (d, 4H) *J*= 8.4 Hz • 7.14 (d, 4H) *J*= 8.6 Hz • 6.96 (d, 8H) *J*= 8.6 Hz	• 8.08 (d, 4H) *J*= 16.6 Hz • 7.53 (d, 4H) *J*= 16.6 Hz	-	• 4.40 (t, 4H) *J*= 7.0 Hz • 4.12 (t, 4H) *J*= 7.5 Hz	-	• 5.29 (s, 4H) • 4.19 (t, 8H) *J*= 4.7 Hz • 3.89 (t, 8H) *J*= 4.7 Hz • 3.77-3.75 (m, 8H) • 3.71-3.69 (m, 8H) • 3.68-3.65 (m, 8H) • 3.57-3.55 (m, 8H)	3.38 (s, 12H)	-	• 1.96 (q, 4H) *J*= 7.1 Hz • 1.73 (q, 4H) *J*= 7.1 Hz	1.47 (m, 20H)

Table S2. FT-IR Parameters of **9**, **10**, **GO-9** and **GO-10**.

Compound	υ_{O-H}	$\upsilon_{C-H(str)}$	$\upsilon_{C=O(str)}$	$\upsilon_{C=C(str)}$	$\upsilon_{B-N(str)}$	$\upsilon_{C-H(bnd)}$	$\upsilon_{C-N(str)}$	$\upsilon_{C-O(str)}$
9	-	2931.34; 2865.67	1711.94	1596.24	1482.84	1370.89	1197.01	1052.98
10	-	2923.13; 2863.43	1701.49	1661.19, 1596.27	1508.95	-	1243.28	1100.75
GO-9	3172.39	2928.36; 2864.18	1702.98	1596.27	1484.33	1367.16	1199.25	1055.22
GO-10	3161.94	2926.86; 2864.92	1703.73	1644.03; 1597.76	1507.46	-	1241.04	1097.01